Catalyst-Free Crosslinking Modification of Nata-De-Coco-Based Bacterial Cellulose Nanofibers Using Citric Acid

Rabiu Salihu
Universiti Teknologi Malaysia - Main Campus Skudai: Universiti Teknologi Malaysia
Saiful Izwan Abd Razak (saifulizwan@utm.my)
Universiti Teknologi Malaysia - Main Campus Skudai: Universiti Teknologi Malaysia
https://orcid.org/0000-0003-1583-9346
Nurliyana Ahmad Zawawi
Universiti Teknologi Malaysia - Main Campus Skudai: Universiti Teknologi Malaysia
Shafinaz Shahir
Universiti Teknologi Malaysia - Main Campus Skudai: Universiti Teknologi Malaysia
Mohd Helmi Sani
Universiti Teknologi Malaysia - Main Campus Skudai: Universiti Teknologi Malaysia
Mohammed Ahmad Wsoo
Universiti Teknologi Malaysia - Main Campus Skudai: Universiti Teknologi Malaysia
Nadirul Hasraf Mat Nayan
Universiti Tun Hussein Onn Malaysia

Research Article

Keywords: Bacterial cellulose, citric acid, catalyst-free, crosslinking, nata-de-coco, biomedicine

Posted Date: May 24th, 2021

DOI: https://doi.org/10.21203/rs.3.rs-519385/v1

Abstract

Bacterial cellulose (BC) has gained research attention in materials science and biomedicine due to its fascinating properties. BCs' fiber collapse phenomenon (inability to reabsorb water after dehydration) is one of the drawbacks that limit its potentials. To overcome this, a catalyst-free thermal crosslinking reaction was employed to modify the BC using citric acid (CA) without compromising the biocompatibility. Properties evaluation of the modified BC (MBC) by FTIR, XRD, SEM/EDX, TGA, and Tensile analysis confirmed the fiber crosslinking and improvement of some properties that could be advantageous for various applications. The modified nanofiber seems to maintain its inherent crystallinity and thermal stability with an increased water absorption/swelling and tensile modulus. The resulting MBC reported here can be relevant for wound dressings and tissue scaffolding.

1. Introduction

The Philippines originated jelly dessert (Nata-de-coco) is the cheapest form of bacterial cellulose (BC) produced through the fermentation of coconut water [1]. It is a pure form of (BC) with unique physicochemical, morphological, and mechanical properties [1, 2]. Owing to this, nata-de-coco-based BC can serve as a good reference point for applications such as biomedicine, where high material purity is a primary demand. Its large-scale production in many Asian countries like Malaysia, Indonesia, and Thailand [3] will not be unconnected with the advantageous ease of the process.

BC is a microfibrillar biomaterial first reported by Andrian Brown in 1886. Different species of bacteria such as *Acetobacter xylinum, Rhizobium, Achromobacter*, and *Sarcina* were reported to produce BC through fermentation [4–6]. BC is generally pure, biocompatible, non-toxic, and has a broad modifying ability into different forms and compositions. This earns it a remarkable range of applications in many fields of science and medicine [7–9]. However, its inability to reabsorb much water after being dehydrated and inadequate functionality limits the said attractiveness, hence the need for its modification [10].

In-situ and ex-situ modifications were principally the major approaches known for BC modification. The ex-situ modification mostly after BCs' production, involves either physical or chemical process [11–13]. One of the methods of interest is the crosslinking reaction (a process that induces a strong linkage between the polymer chains through covalent bonding), owing to its simplicity and effectiveness [14].

CA is one of the organic acids enlisted as generally regarded as safe (GRAS) by the US food and drug administration (FDA) that has long been used as modifier on many polymeric biomaterials via crosslinking, including the BC [15–19]. Modification of polymeric biomaterial with CA mostly yielded what is also known as citrate-based biomaterial (CBB) [20, 21]. Owing to their excellent biological, chemical, and material properties, such as antimicrobial, antioxidant, and fluorescence properties, CBBs have been trending in biomedicine [22–24]. Crosslinking a biopolymer with CA requires an elevated temperature of 120–190 ºC [25]. This method offers the advantage of fine-tuning the material properties such as mechanical, chemical, and degradation properties [26, 27].

CA crosslinking of biopolymers involving different catalysts has been reported by many scientist, but the undesirable effects posed by the catalysts [28, 29] may limit their application in biomedicine. We, therefore, hypothesised that "the use of the catalyst for BCs' crosslinking modification is unnecessary". In this study, a catalyst-free thermal crosslinking approach was employed for the first time to modify the nata-de-coco-based BC fibers using a readily available and inexpensive multifunctional monomer, the CA The physicochemical, morphological, and mechanical properties evaluation of the resulting biopolymer showed that it retained most of its important properties such as crystallinity and thermal stability and improved water absorption rate and tensile modulus compared to the unmodified. Our method seems to be the cheapest and easiest approach that yields promising improvements of BCs' properties and showed that the use of the catalyst for BCs' modification might be unnecessary.

2. Materials And Methods

Bacterial cellulose (BC) sheets were purchased from a local Nata-de-Coco company (Happy Alliance). Citric acid (CA) monohydrate powder ($C_6H_8O_7.H_2O$) and Sodium hydroxide (NaOH) were all purchased from Merck (Sigma-Aldrich).

2.1 Purification and Modification of BC

BC hydrogels were modified with CA by thermal crosslinking as in [30] with slight modification to exclude the catalyst. Briefly, the wet BC sample was cut into 100 mm x 50 mm and purified in 1% (w/v) NaOH at 90 ºC for 60 mins then washed with distilled water until the pH becomes 7–8 at 37 ºC. BC sheets were immersed in different molar (M) concentrations (0.0375, 0.075, 0.15, 0.3 and 0.6) of CA solution in ion-exchanged distilled water (diH_2O) and allowed to stand for 24 hrs at 45 ºC then cured in an oven at 140 ºC for 2 hrs. The same dimension of BC was treated under the same condition in diH_2O only as a control sample. Samples were then removed and rinsed with diH_2O until the pH is 5–6, then tagged as BC (pristine), MBC0.03 (0.0375M), MBC0.07 (0.075M), MBC0.15 (0.15M), MBC0.30 (0.3M), and MBC0.60 (0.6M), and freeze-dried for characterisation.

2.2 Characterisation

For comparison, the BC films were characterised based on physicochemical, morphological, and mechanical properties through scanning electron microscopy (SEM), energy dispersive X-ray (EDX), fourier transform infrared (FTIR), X-ray diffraction (XRD), water contact angle (WCA), swelling rate (SR), thermogravimetric analysis (TGA) and tensile modulus.

2.2.1 Scanning Electron Microscopy (SEM.)

The surface morphology of the fibers before and after modification was examined by SEM analysis (Model: Hitachi TM3000, Japan) equipped with an (EDX) system. Micrographs of platinum sputter-coated were taken at an accelerating voltage of 15 kV for different magnifications. Full-scale elemental quantification data were also acquired from the EDX system.

2.2.2 Fourier Transformed Infrared (FTIR)

The BC, MBC samples were analysed using (Model: PerkinElmer-Frontier™, L1280044, USA) spectrophotometer equipped with an attenuated total reflection (ATR-FTIR) system as in [31]. The spectra were obtained from scans between a wavelength range of 4000 to 650 cm^{-1} and 4 cm^{-1} resolution.

2.2.3 X-ray Diffraction (XRD)

The XRD analysis was performed using (Model: Rigaku SmartLab, U.S.A.) X-ray diffractometer with CuKα radiation wavelength (λ = 0.154 nm) operated at 40 kV and 30 mA. Scans were made between angle *2θ* of 10 º to 60 º at a speed of 3 º/min. The crystallinity index (*CrI*), the crystallite size (CS) and crystal allomorphs of cellulose I were calculated from the data using equations 1, 2 & 3, respectively [32].

$$CrI(\%) = I_{200} - I_{am}/I_{200}\, x\, 100 \quad (1)$$

Where I_{200} represents the maximum intensity of the diffraction peak at (200) lattice plane and I_{am} represents the diffraction intensity at 2θ = 18 º corresponding to the amorphous region of BC.

$$CS = K\lambda/FWHM cos\theta \quad (2)$$

K is the Scherrer's constant (0.9), λ is the X-ray wavelength (1.54Å), FWHM is the width of the diffraction peak at maximum height, and θ is the Bragg's angle.

$$Z = 1693d_1 - 902d_2 - 594 \quad (3)$$

The term Z denotes discriminant function developed by [33], d_1 is the d-spacing of 1–10 peak, and d_2 is the d-spacing of 110 peaks. Where $Z > 0$ or $Z < 0$ indicates I_α or I_β rich type of cellulose, respectively [34].

2.2.4 Water Contact Angle (WAC.)

Water contact angle (WCA.) Optima machine (Model: 1020046094) equipped with a camera was used to capture the water droplet image and measure the contact angle. Briefly, 20 x 20 mm sheets were cut after freeze-drying before the process. A uniform droplet of 2.0 µl of deionised water (diH_2O) was dispensed on five (5) different points on each sample, and an average angle was then recorded [35].

2.2.5 Swelling rate (SR.)

Freeze-dried samples were cut into 30 x 30 mm, the dried weight (W_1) recorded, then immersed in either distilled water or SBF at ambient temperature. Samples were then removed and weighed at certain intervals after been blotted with a filter paper to remove the excess water until an equilibrium weight (W_2) is reached. The swelling rate was calculated using Eq. 4 below [36, 37].

$$SR = W_2 - W_1/W_1 \, x \, 100 \quad (4)$$

Where W_1 is the dried weight and W_2 is the final wetted weight.

2.2.6 Thermal Gravimetric Analysis (TGA)

The thermal stability of all samples was evaluated using a thermal analyser (Shimadzu DTG-60H, Japan). A freeze-dried film weighing 18 mg ± 3 mg for all the samples in a platinum pan was heated between 30 ºC and 900 ºC at 10 ºC/min heating rate under a nitrogen atmosphere of 100 ml/min flow rate. The weight loss upon heating was normalised as percentage weight loss (%) and plotted against the corresponding temperature (ºC) [38].

2.2.7 Tensile properties

Tensile properties of the BC and MBC samples were evaluated using a tensile testing machine (Zwick/Roell Z020, Zwick, Germany) according to ASTM-D882 standards. Briefly, freeze-dried samples kept in a desiccator were cut into a rectangular shape (70 x 20 mm) with different thickness. A "gauze" length of 50 mm was used, and all measurements were performed for at least five samples at a crosshead speed of 2 mm/min [39, 40] in an ambient condition.

3. Results And Discussion

3.1 Scanning Electron Microscopy (SEM/EDX)

From the SEM micrographs shown in figure 1, cellulose fibers can be observed with different surface morphologies among the samples. The unmodified sample (BC) appears to have a compacted fiber network with uniformly interconnected pores similar to what [41] reported. The modified samples, on the other hand, displayed different fiber networks depending on the CA concentration. At lower concentrations (MBC0.03, MBC0.07 and MBC0.15), porous fiber networks can be observed that could allow for more water absorption. The higher concentration (MBC0.30 and MBC0.70), in contrast, showed a bit compacted fiber similar to the untreated sample. This could be due to the high crosslinking density that occurs between the fibers, thus affecting the porosity and preventing the passage of water molecules leading to a low swelling rate, as explained in **Section 3.5** and Figure 7.

The EDX spectra in Figure 2 represents the elemental composition (Carbon and Oxygen) typical of organic fiber, while the elemental and atomic weight percentages were presented in Table 1 for the pure and modified BC.

The slight shift of the elemental and atomic weight percentage (Table 1) of both carbon and oxygen in the pure sample (BC) in comparison is logically indicating the presence of CA in all modified samples. CA having the chemical formula ($C_6H_8O_7$), have added to/compensated the percentage of oxygen atoms in the pure BC having the chemical formula $(C_6H_{10}O_5)_n$, thus reducing the proportion of carbon and increasing that of oxygen, similar to the trend reported for ascorbic acid modification on cellulose by [42].

The EDX data showing the carbon (C) and oxygen (O) peaks only (Figure 2) is also suggesting the notion that nata-de-coco-based BC is highly (~99%) pure [43].

3.2 Fourier Transformed Infrared (FTIR)

The FTIR spectra of the pristine and modified samples were shown in Figure 3. The signature peaks attributed to the dominant functional group of BCs' (OH-stretching) vibration were at 3346 cm^{-1}. Peaks obtained at 2865 cm^{-1} and 1420 cm^{-1} were due to C-H stretching and 1450 cm^{-1} due to CH_2 absorptions. Peaks obtained at 1719 cm^{-1} related to carbonyl/carboxyl (C=O) stretching [44] appears only on the crosslinked samples thus, confirming the presence of CA within the modified BC samples [30, 45, 46]. Peaks between 1055 cm^{-1}, 1020 cm^{-1} were due to C-O-C interactions. The reduced intensity of the OH peaks on the crosslinked samples can also result from the chemical interaction with CA [47]. Overall, the low intense OH peaks at 3346 cm^{-1} and 1711 cm^{-1} on treated samples are indications that crosslinking modification on the BC was successful. The proposed mechanism of CA crosslinking on BC was presented in a schematic diagram in Figure 4.

3.3 X-ray Diffraction (XRD)

XRD patterns shown in Figure 5 represents the spectra obtained for the pure, modified samples. All samples showed peaks typical of cellulose *I* allomorph at lattice planes of 110, 1-10, and 200 corresponding to 2θ values of 14.6 º, 16.6 º, and 22.6 º, respectively as previously reported [32, 34, 48, 49]. Distinctive peaks with different intensities obtained at diffraction planes of 130, 042 and 040 corresponding to 2θ values of 19.4 º, 26.1 º and 34.3 º appear only on the modified samples, thus attributed to the CA crosslinking of the BC [50].

The peaks associated with BCs' crystallinity appear with similar intensities for all the samples, indicating that the CA modification has less effect on the crystalline structure and morphology of the BC [51, 52]. Even though [15] reported a decrease in crystalline peaks on sodium carboxymethylcellulose (NaCMC) crosslinked with CA, such may likely be due to one of the cellulose derivatives. De Lima et al. suggested that the decreased crystallinity they observed is ascribed to the viscosity increase of NaCMC or its interaction with cellulose nanofibers during crystallisation [53].

The crystallinity index and crystallite size values calculated from the XRD data were between 92% to 95% and 51Å to 56Å. This essentially shows that the CA crosslinking has less effect on the crystallinity and crystallite size of the MBC. Furthermore, cellulose *I* allomorph calculated using the *Z*-discriminant function also showed that all the samples have the same cellulose *Ia* rich (triclinic) form, the typical of bacterial cellulose [54, 55]. All calculated agreed with previously reported data [30] and indicate that the BC still maintained its crystalline nature after the crosslinking modification.

3.4 Water Contact Angle (WCA.)

The wetting behaviour of a materials' surface is closely related to the molecular terminal groups present, and contact angle studies give information on the wettability properties of a material [56]. In theory, a surface is considered hydrophilic or super hydrophilic when its WCA is smaller than 90º or 10º, respectively [35]. Figure 6 represents the mean contact angle measured for the pure and modified BC samples. All, including the pure BC, fall between 0º and 33.90º, signifying that all samples were either hydrophilic or super hydrophilic depending on their contact angles. However, it noteworthy that the modified samples have shown a decreasing WCA up to 0º (MBC0.30 and MBC0.60) where the water droplet is no longer capturable (disperses as soon as dropped). BC's hydrophilicity could be attributed to the additional carboxyl groups [44, 57] that can form hydrogen bonds with water molecules [58]. Even though a native BC is inherently hydrophilic, the angle of contact with water tends to decrease with increasing the CA concentration. Essentially here, the CA modification on BC has improved its surface chemistry to attract more water further.

3.5 Swelling rate (SR.)

Generally, polymeric materials' water absorption and swelling behaviour are through capillary action and diffusion and electrostatic repulsion between the ions on the polymer chains that forces it to expand and swell [57]. The swelling rate (SR) for the pure and modified BC samples was presented in Figure 7. Modified samples have shown an increased SR, mostly at lower and decrease higher concentrations of CA to a rate even below that of the pure BC. The decrease in SR with the increase in CA concentration could be due to the numerous crosslinker points formed within the BCs' fiber networks, thus reducing the spaces for water to enter [57]. It is evident for samples (MBC0.30 and MBC0.60) having the lowest absorption rates, a packed fiber geometry on the SEM micrographs in Figure 1, and the sample images in figure 7, which could result from the high concentration of CA Water absorption/swelling is especially advantageous for BCs' medical applications, such as wound dressings [28]. Interestingly, all samples showed similar SR in both SBF and DI water. The SR results reported here agreed with the previous report that BC water holding capacity is between 60 to 700 times its dry weight [59].

3.6 Thermal Gravimetric Analysis (TGA)

An important property of BC is its thermal stability, especially for applications in biomedicine where higher temperatures are applied for sterilisation processes. Figure 8 shows the thermal behavior of the pristine and modified BC evaluated in this study. An initial weight loss observed for all the samples at a temperature between 45 to 120 ºC was due to absorbed moisture evaporation. Except for samples with the highest CA concentration (MBC0.30 and MBC0.60) that displayed a partial decomposition between 120 to 300 ºC, all other modified samples were not different from the pristine BC. They all showed a maximum weight loss at a temperature between 300 to 392 ºC due to dehydration, decomposition, and dissociation of the glycosidic linkages [60-62]. The partial, total and residual mass loss observed at maximum temperatures 300 ºC, 392 ºC, and 620.93 ºC were 25.928%, 88.149%, and 7.875%, respectively. The partial decomposition observed may also be due to the high concentration of CA that attracts more

moisture than the lower concentrations. Our result implies that the CA modification has less effect on the thermal properties of the BC [63].

3.7 Tensile Testing

Table 2 represents the tensile test results for all the samples with the modified showing improved mechanical strength compared to the unmodified, except for the lowest CA concentration (MBC0.03), which exhibits a very low tensile strength value. The decrease in the mechanical strength displayed could result from lesser crosslinking degrees within the fiber networks due to the low amount of the crosslinker, which can also be seen from the SEM micrographs Figure 1. The sample thickness and spongy appearance after freeze-drying could also lead to the loosening of the fibers. It can also be observed that, despite having a lower modulus value, the elongation at break is within the same range as other modified samples, implying that the elasticity of the fibers is close to other modified samples after reaching the maximum yield limit.Like the modulus, the tensile strength also follows the trend as increasing with the CA concentration if not for the lowest concentration. However, the elongation at break showed a different pattern where it increases from the lowest and decreases at the highest concentration, especially in the lowest concentration. Therefore, it can be hypothesised that high concentration CA treatment on BC may have a negative effect on the stretching ability of the BC fiber.

4. Conclusion

Several attempts to enhance BCs' properties through crosslinking modification involve the use of catalysts. Some of these catalysts might alter the chemical composition and compromise the resulting polymer's biocompatibility, limiting its application, especially in biomedicine. Here we reported for the first time a catalyst-free modification of BC with CA through a simple immersion hydrothermal crosslinking. The improvements in the chemical, morphological, thermal, and mechanical properties presented in this report are an indication that the modification has resulted in a potential citrate-based biopolymer that can be used as future wound dressings or a tissue scaffold material. The approach used here seems to be the cheapest and easiest modification method that yielded some promising results. Thus, it portrayed effectiveness and showed that catalyst might be excluded for future BC modification, especially when intended for biomedical applications, and, therefore, support our hypothesis.

Declarations

The authors are unequivocally and solemnly declaring that the manuscript has not been published elsewhere and is not under consideration by any other journal. There is no conflict of interest regarding the article.

Data Availability

All data generated or analysed during the study are included in this article and are available from the corresponding author on reasonable request.

References

1. Nugroho, D.A. and P. Aji, *Characterization of nata de coco produced by fermentation of immobilized Acetobacter xylinum.* Agriculture and Agricultural Science Procedia, 2015. **3**: p. 278-282.
2. Phisalaphong, M., et al., *Nata de coco industry in Vietnam, Thailand, and Indonesia*, in *Bacterial nanocellulose*. 2016, Elsevier. p. 231-236.
3. Halib, N., M. Amin, and I. Ahmad, *Physicochemical properties and characterization of nata de coco from local food industries as a source of cellulose.* Sains Malaysiana, 2012. **41**(2): p. 205-211.
4. Brown Jr, R.M., *Cellulose structure and biosynthesis: what is in store for the 21st century?* Journal of Polymer Science Part A: Polymer Chemistry, 2004. **42**(3): p. 487-495.
5. Jonas, R. and L.F. Farah, *Production and application of microbial cellulose.* Polymer degradation and stability, 1998. **59**(1-3): p. 101-106.
6. Shoda, M. and Y. Sugano, *Recent advances in bacterial cellulose production.* Biotechnology and Bioprocess Engineering, 2005. **10**(1): p. 1.
7. Pang, M., et al., *Application of bacterial cellulose in skin and bone tissue engineering.* European Polymer Journal, 2020. **122**: p. 109365.
8. Tayeb, A.H., et al., *Cellulose Nanomaterials—Binding Properties and Applications: A Review.* Molecules, 2018. **23**(10): p. 2684.
9. Ahmed, J., M. Gultekinoglu, and M. Edirisinghe, *Bacterial cellulose micro-nano fibres for wound healing applications.* Biotechnology Advances, 2020: p. 107549.
10. Naeem, M.A., et al., *Insitu self-assembly of bacterial cellulose on banana fibers extracted from peels.* Journal of Natural Fibers, 2020. **17**(9): p. 1317-1328.
11. Stumpf, T.R., et al., *In situ and ex situ modifications of bacterial cellulose for applications in tissue engineering.* Materials Science and Engineering: C, 2018. **82**: p. 372-383.
12. Ul-Islam, M., T. Khan, and J.K. Park, *Water holding and release properties of bacterial cellulose obtained by in situ and ex situ modification.* Carbohydrate Polymers, 2012. **88**(2): p. 596-603.
13. Salihu, R., et al., *Overview of inexpensive production routes of bacterial cellulose and its applications in biomedical engineering.*
14. Oryan, A., et al., *Chemical crosslinking of biopolymeric scaffolds: Current knowledge and future directions of crosslinked engineered bone scaffolds.* International journal of biological macromolecules, 2018. **107**: p. 678-688.
15. Dharmalingam, K. and R. Anandalakshmi, *Fabrication, characterization and drug loading efficiency of citric acid crosslinked NaCMC-HPMC hydrogel films for wound healing drug delivery applications.* International journal of biological macromolecules, 2019. **134**: p. 815-829.
16. Cumming, M.H., et al., *Intra-fibrillar citric acid crosslinking of marine collagen electrospun nanofibres.* International Journal of Biological Macromolecules, 2018. **114**: p. 874-881.

17. Ren, L., et al., *Convenient Method for Enhancing Hydrophobicity and Dispersibility of Starch Nanocrystals by Crosslinking Modification with Citric Acid.* International Journal of Food Engineering, 2018. **14**(4): p. 20170238.
18. Sedyakina, N., et al., *Modulation of Entrapment Efficiency and In Vitro Release Properties of BSA-Loaded Chitosan Microparticles Cross-Linked with Citric Acid as a Potential Protein–Drug Delivery System.* Materials, 2020. **13**(8): p. 1989.
19. Uranga, J., et al., *The Effect of Cross-Linking with Citric Acid on the Properties of Agar/Fish Gelatin Films.* Polymers, 2020. **12**(2): p. 291.
20. Salihu, R., et al., *Citric Acid: A Green Cross-linker of Biomaterials for Biomedical Applications.* European Polymer Journal, 2021: p. 110271.
21. Ma, C., et al., *Citrate-based materials fuel human stem cells by metabonegenic regulation.* Proceedings of the National Academy of Sciences, 2018. **115**(50): p. E11741-E11750.
22. Shah, A.H., et al., *Twin screw extrusion of conductive citrate-based biomaterials.* European Polymer Journal, 2019. **110**: p. 176-182.
23. Sabzi, M., et al., *pH-dependent swelling and antibiotic release from citric acid crosslinked poly (vinyl alcohol)(PVA)/nano silver hydrogels.* Colloids and Surfaces B: Biointerfaces, 2020. **188**: p. 110757.
24. Huang, L., et al., *Targeting citrate as a novel therapeutic strategy in cancer treatment.* Biochimica et Biophysica Acta (BBA)-Reviews on Cancer, 2020. **1873**(1): p. 188332.
25. Khouri, J., *Chitosan Edible Films Crosslinked by Citric Acid*. 2019, University of Waterloo: Waterloo, Ontario, Canada, 2019. p. 188.
26. Tran, R.T., J. Yang, and G.A. Ameer, *Citrate-based biomaterials and their applications in regenerative engineering.* Annual review of materials research, 2015. **45**: p. 277-310.
27. Ma, C., et al., *Citrate chemistry and biology for biomaterials design.* Biomaterials, 2018. **178**: p. 383-400.
28. Ciecholewska-Jusko, D., et al., *Superabsorbent crosslinked bacterial cellulose biomaterials for chronic wound dressings.* bioRxiv, 2020.
29. Feng, X., et al., *Esterification of wood with citric acid: The catalytic effects of sodium hypophosphite (SHP).* Holzforschung, 2014. **68**(4): p. 427-433.
30. Meftahi, A., et al., *Preventing the collapse of 3D bacterial cellulose network via citric acid.* Journal of Nanostructure in Chemistry, 2018. **8**(3): p. 311-320.
31. Bilgi, E., et al., *Optimization of bacterial cellulose production by Gluconacetobacter xylinus using carob and haricot bean.* International journal of biological macromolecules, 2016. **90**: p. 2-10.
32. Khan, H., A. Kadam, and D. Dutt, *Studies on bacterial cellulose produced by a novel strain of Lactobacillus genus.* Carbohydrate Polymers, 2020. **229**: p. 115513.
33. Wada, M., T. Okano, and J. Sugiyama, *Allomorphs of native crystalline cellulose I evaluated by two equatoriald-spacings.* Journal of Wood Science, 2001. **47**(2): p. 124-128.

34. Poletto, M., H.L. Ornaghi, and A.J. Zattera, *Native Cellulose: Structure, Characterization and Thermal Properties.* Materials (Basel), 2014. **7**(9): p. 6105-6119.
35. Zhao, T. and L. Jiang, *Contact angle measurement of natural materials.* Colloids and Surfaces B: Biointerfaces, 2018. **161**: p. 324-330.
36. Shao, W., et al., *Construction of silver sulfadiazine loaded chitosan composite sponges as potential wound dressings.* Carbohydrate polymers, 2017. **157**: p. 1963-1970.
37. Ye, S., et al., *Development of gelatin/bacterial cellulose composite sponges as potential natural wound dressings.* International journal of biological macromolecules, 2019. **133**: p. 148-155.
38. Abba, M., et al., *Physicochemical, Morphological, and Microstructural Characterisation of Bacterial Nanocellulose from Gluconacetobacter xylinus BCZM.* Journal of Natural Fibers, 2020: p. 1-12.
39. Tang, S., et al., *A covalently cross-linked hyaluronic acid/bacterial cellulose composite hydrogel for potential biological applications.* Carbohydrate Polymers, 2020. **252**: p. 117123.
40. Molina-Romero, J.M., et al., *Reduced tensile properties of bacterial cellulose membranes after an accelerated composite temperature/humidity cyclic assay.* Journal of Polymers and the Environment, 2021: p. 1-10.
41. Rathinamoorthy, R., et al., *Development and Characterization of Self-assembled Bacterial Cellulose Nonwoven Film.* Journal of Natural Fibers, 2019: p. 1-14.
42. Ibrahim, N.A., et al., *Environmentally sound approach for imparting antibacterial and UV-protection functionalities to linen cellulose using ascorbic acid.* International journal of biological macromolecules, 2019. **135**: p. 88-96.
43. Blanco Parte, F.G., et al., *Current progress on the production, modification, and applications of bacterial cellulose.* Critical Reviews in Biotechnology, 2020. **40**(3): p. 397-414.
44. Pandit, A. and R. Kumar, *A Review on Production, Characterization and Application of Bacterial Cellulose and Its Biocomposites.* Journal of Polymers and the Environment, 2021: p. 1-18.
45. Wu, Y.-L., et al., *Enhanced metal ion rejection by a low-pressure microfiltration system using cellulose filter papers modified with citric acid.* ACS applied materials & interfaces, 2018. **10**(38): p. 32736-32746.
46. Haji, A., S.M. Bidoki, and F. Gholami, *Isotherm and Kinetic Studies in Dyeing of Citric Acid-Crosslinked Cotton with Cationic Natural Dye.* Fibers and Polymers, 2020. **21**(11): p. 2547-2555.
47. Raucci, M., et al., *Effect of citric acid crosslinking cellulose-based hydrogels on osteogenic differentiation.* Journal of Biomedical Materials Research Part A, 2015. **103**(6): p. 2045-2056.
48. Trovatti, E., et al., *Gluconacetobacter sacchari: An efficient bacterial cellulose cell-factory.* Carbohydrate Polymers, 2011. **86**(3): p. 1417-1420.
49. Bagheri, M., et al., *Application of chitosan-citric acid nanoparticles for removal of chromium (VI).* International Journal of Biological Macromolecules, 2015. **80**: p. 431-444.
50. Ramírez, J.A.Á., et al., *Acetylation of bacterial cellulose catalyzed by citric acid: Use of reaction conditions for tailoring the esterification extent.* Carbohydrate polymers, 2016. **153**: p. 686-695.

51. Ramírez, J.A.Á., et al., *Simple citric acid-catalyzed surface esterification of cellulose nanocrystals.* Carbohydrate polymers, 2017. **157**: p. 1358-1364.
52. Chen, H., et al., *Citric acid/cysteine-modified cellulose-based materials: green preparation and their applications in anticounterfeiting, chemical sensing, and UV shielding.* ACS Sustainable Chemistry & Engineering, 2017. **5**(12): p. 11387-11394.
53. De Lima Fontes, M., et al., *Effect of in situ modification of bacterial cellulose with carboxymethylcellulose on its nano/microstructure and methotrexate release properties.* Carbohydrate Polymers, 2018. **179**: p. 126-134.
54. Zugenmaier, P., *History of cellulose research.* Crystalline cellulose and derivatives: Characterization and structures, 2008: p. 7-51.
55. Moon, R.J., et al., *Cellulose nanomaterials review: structure, properties and nanocomposites.* Chemical Society Reviews, 2011. **40**(7): p. 3941-3994.
56. Giridhar, G., R. Manepalli, and G. Apparao, *Contact Angle Measurement Techniques for Nanomaterials*, in *Thermal and Rheological Measurement Techniques for Nanomaterials Characterization*. 2017, Elsevier. p. 173-195.
57. Luo, M.-T., et al., *Cellulose-based absorbent production from bacterial cellulose and acrylic acid: Synthesis and performance.* Polymers, 2018. **10**(7): p. 702.
58. Lawal, O.S., et al., *Hydrogels based on carboxymethyl cassava starch cross-linked with di-or polyfunctional carboxylic acids: Synthesis, water absorbent behavior and rheological characterizations.* European Polymer Journal, 2009. **45**(12): p. 3399-3408.
59. Portela, R., et al., *Bacterial cellulose: a versatile biopolymer for wound dressing applications.* Microbial biotechnology, 2019. **12**(4): p. 586-610.
60. Chen, W.-H., et al., *Independent parallel pyrolysis kinetics of cellulose, hemicelluloses and lignin at various heating rates analyzed by evolutionary computation.* Energy Conversion and Management, 2020. **221**: p. 113165.
61. Vasconcelos, N.F., et al., *Bacterial cellulose nanocrystals produced under different hydrolysis conditions: Properties and morphological features.* Carbohydrate polymers, 2017. **155**: p. 425-431.
62. Amin, M.C.I.M., A.G. Abadi, and H. Katas, *Purification, characterization and comparative studies of spray-dried bacterial cellulose microparticles.* Carbohydrate polymers, 2014. **99**: p. 180-189.
63. Awadhiya, A., et al., *Synthesis and characterization of agarose–bacterial cellulose biodegradable composites.* Polymer Bulletin, 2017. **74**(7): p. 2887-2903.

Tables

Table 1 Elemental and atomic weight % of samples obtained from EDX analysis

Samples	Weight %		Atomic %	
	Carbon	Oxygen	Carbon	Oxygen
BC	66.5	33.5	72.6	27.4
MBC0.03	59.9	40.1	66.6	33.4
MBC0.07	59.1	40.9	65.8	34.2
MBC0.15	56.9	43.1	63.8	36.2
MBC0.30	62.1	37.9	68.5	31.5
MBC0.60	57.1	42.9	64.0	36.0

Table 2 Mechanical properties of the unmodified and modified samples as mean ± standard deviation

Samples	Thickness (mm)	E_t (MPa)	σ_M (MPa)	ε_B (%)
BC	0.99 ± 0.07	56.68 ± 7.81	1.25 ± 0.16	1.94 ± 0.06
MBC0.03	2.16 ± 0.19	17.97 ± 1.48	0.62 ± 0.16	3.97 ± 0.60
MBC0.07	0.16 ± 0.01	473.59 ± 62.02	20.60 ± 3.58	4.87 ± 0.25
MBC0.15	0.12 ± 0.01	778.42 ± 132.47	28.43 ± 3.15	4.11 ± 0.59
MBC0.30	0.08 ± 0.01	945.73 ± 199.62	26.65 ± 10.13	3.27 ± 0.71
MBC0.60	0.18 ± 0.09	1024 ± 44.66	16.37 ± 0.63	3.23 ± 0.36

Figures

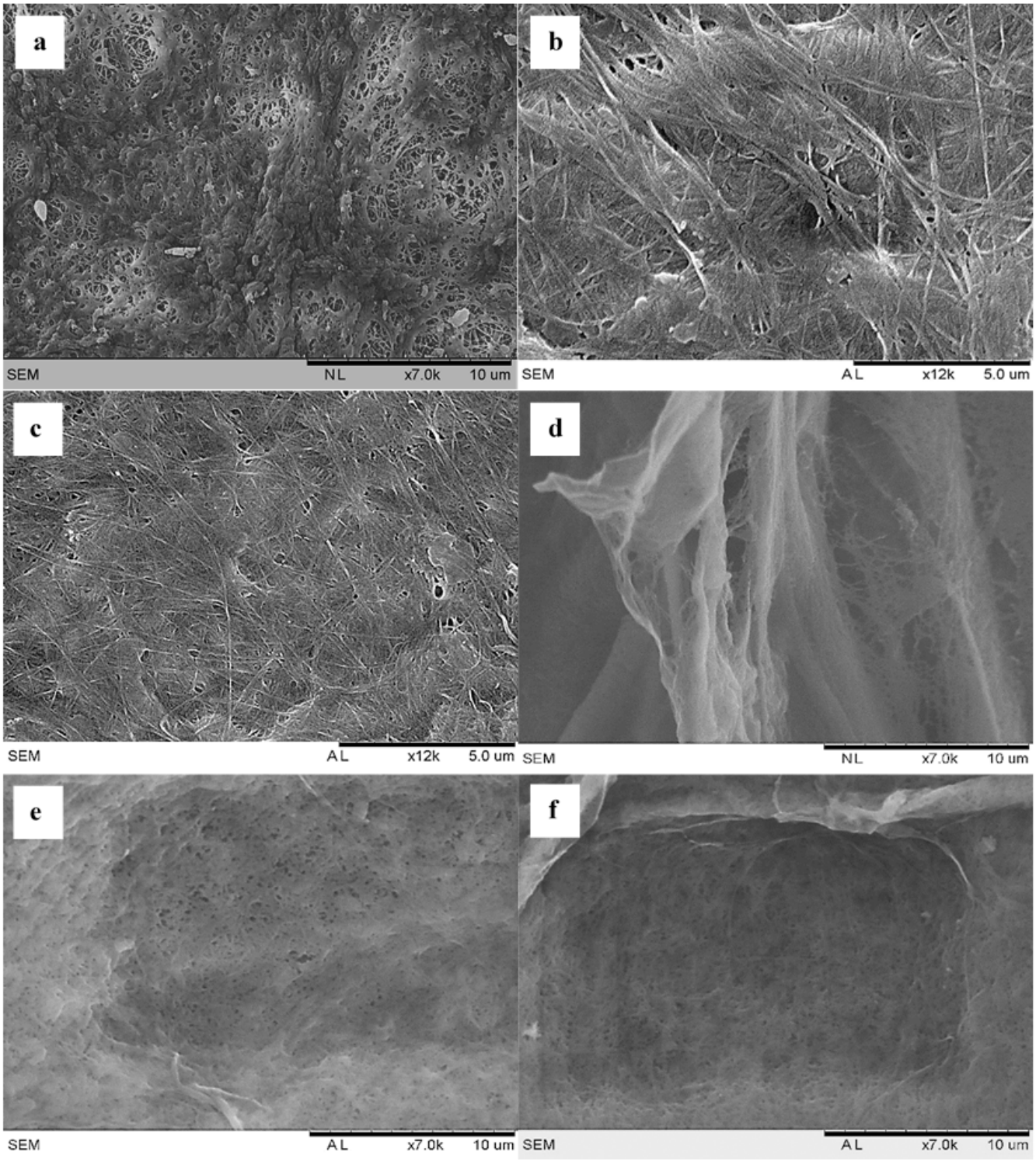

Figure 1

SEM images for (a) BC, (b) MBC0.03, (c) MBC0.07, (d) MBC0.15, (e) MBC0.30, and (f) MBC0.60

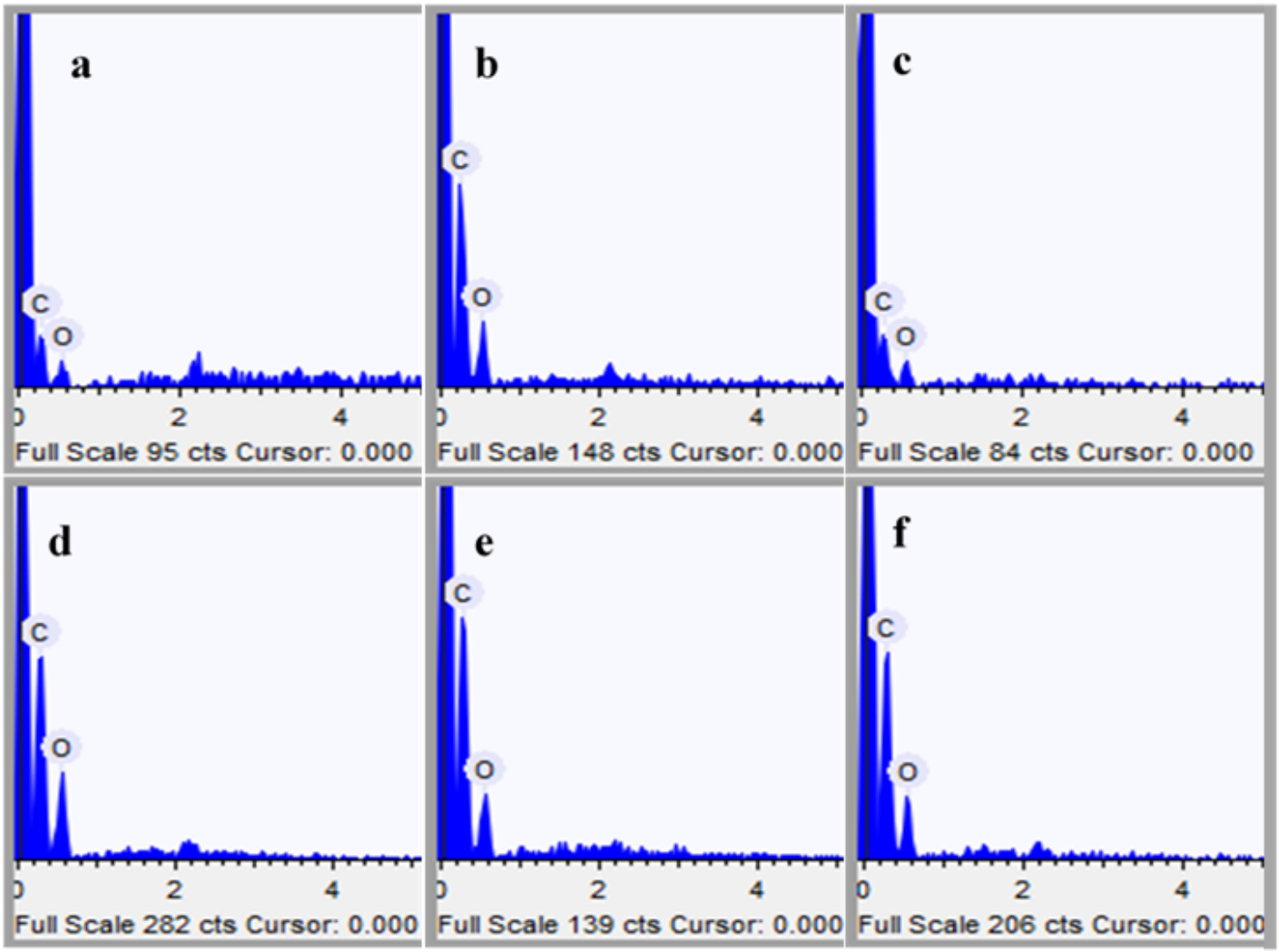

Figure 2

EDX spectral peaks for (a) BC, (b) MBC0.03, (c) MBC0.07, (d) MBC0.15, (e) MBC0.30, and (f) MBC0.60

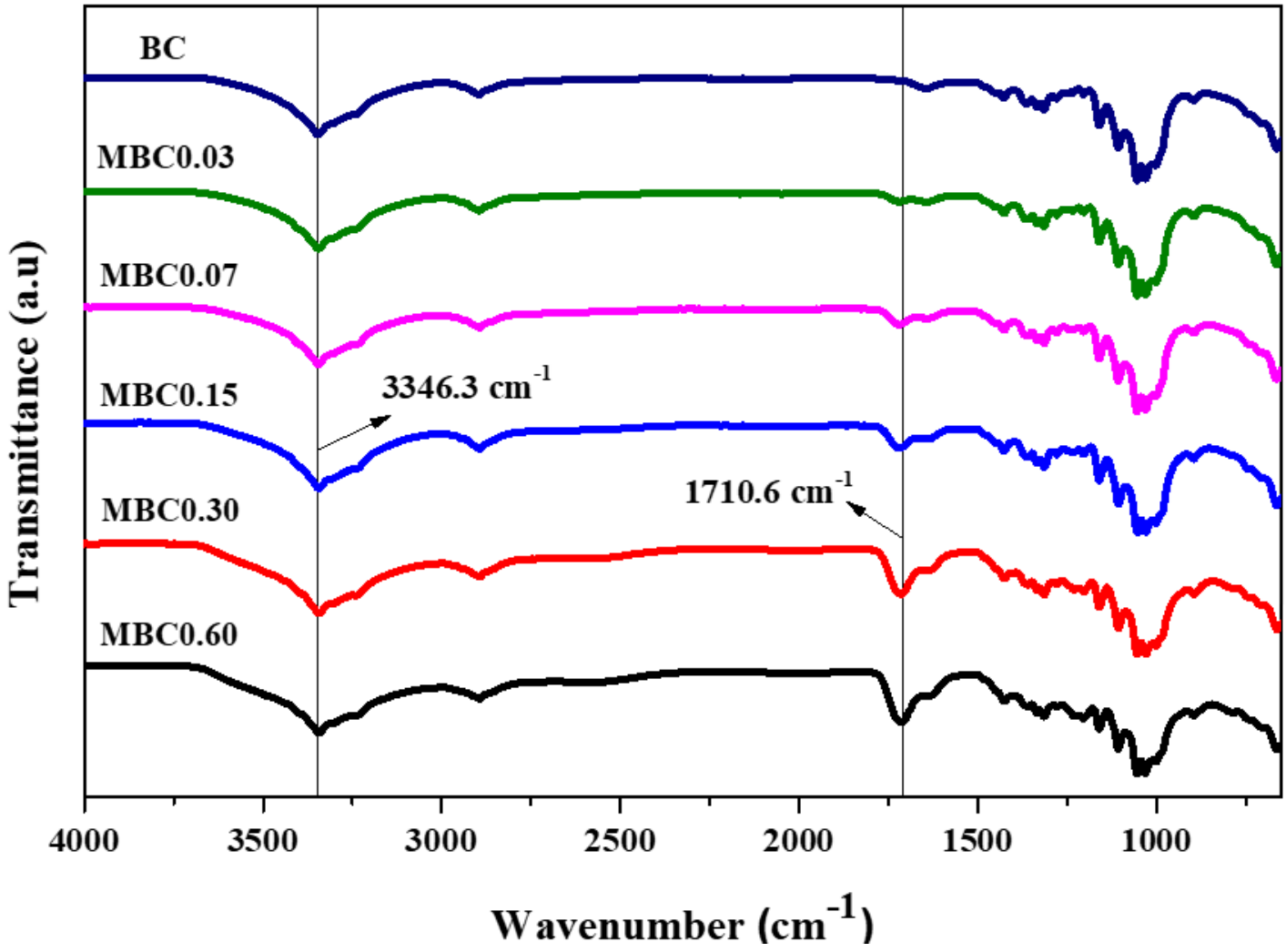

Figure 3

FTIR spectrum of the unmodified and modified samples at different CA concentrations

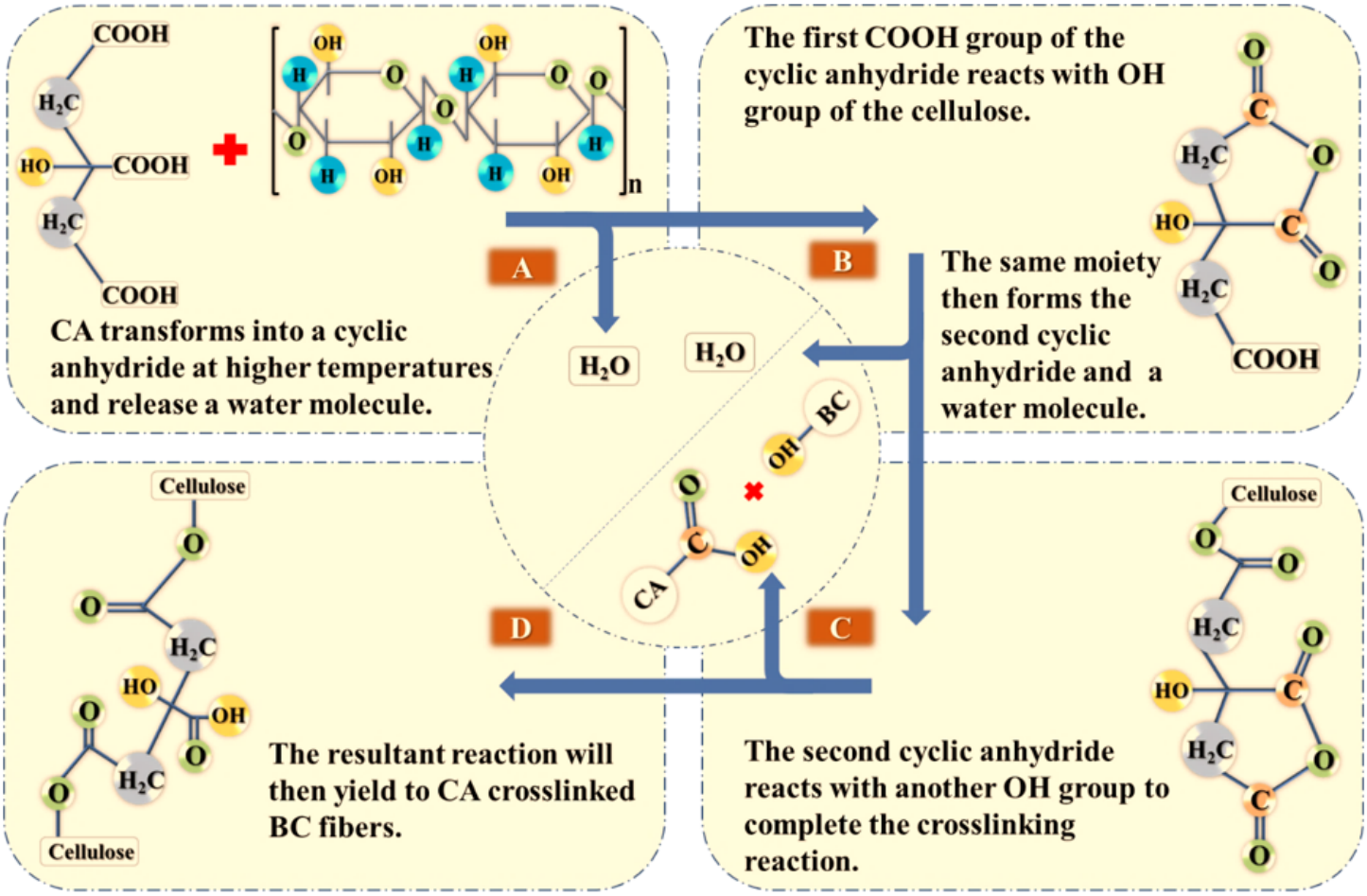

Figure 4

Schematic diagram of the proposed CA crosslinking mechanism on BC

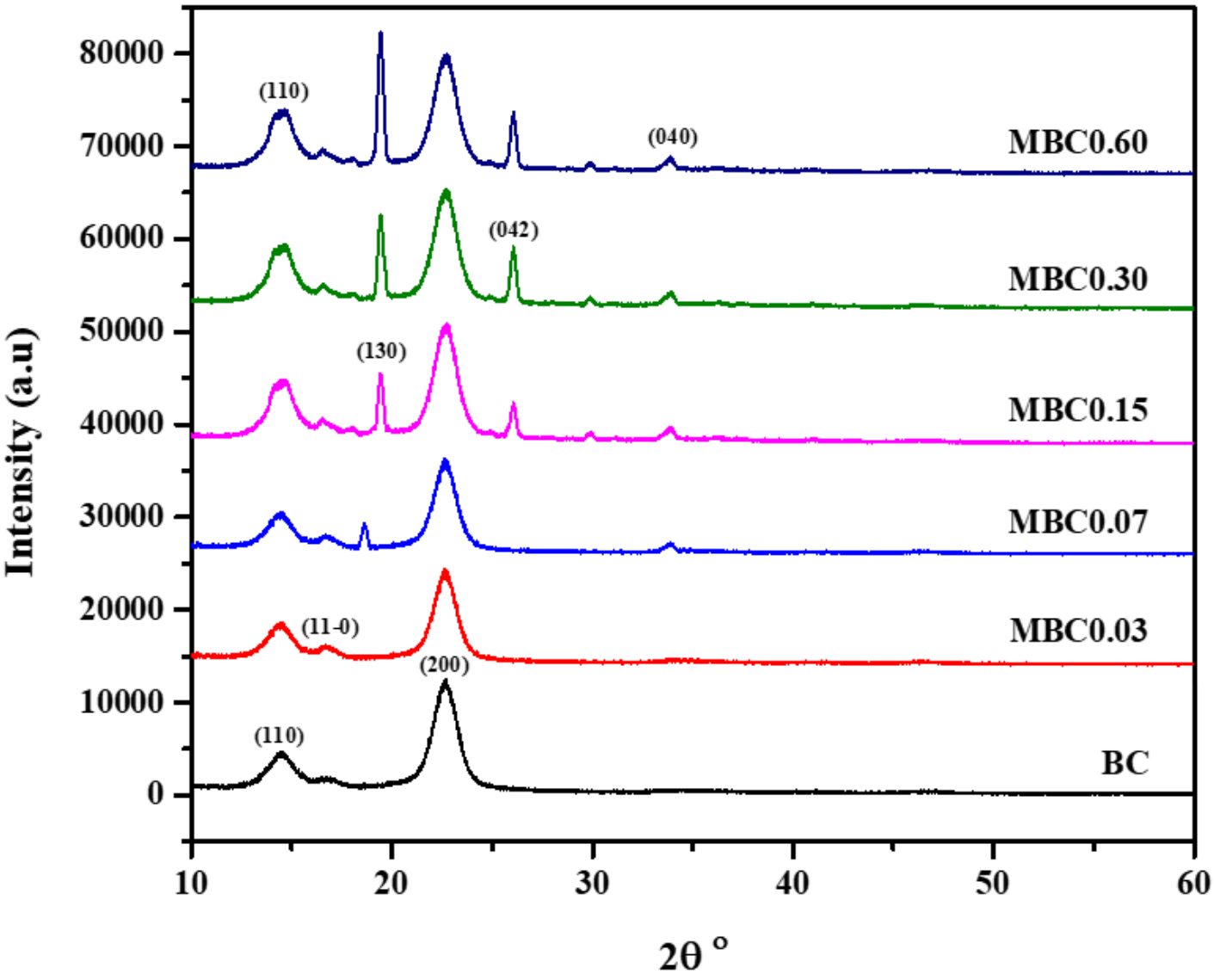

Figure 5

XRD spectra of the unmodified and modified BC

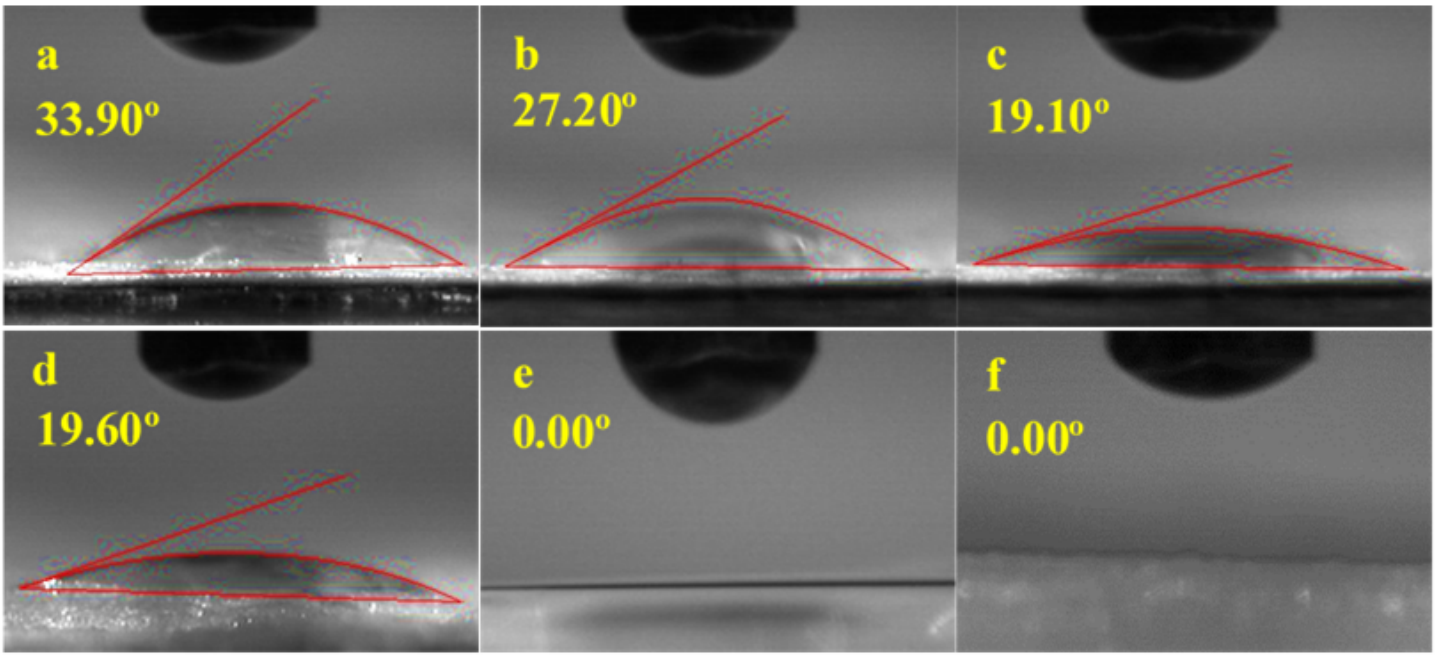

Figure 6

Mean water contact angles obtained for (a) BC, (b) MBC0.03, (c) MBC0.07, (d) MBC0.15, (e) MBC0.30, and (f) MBC0.60

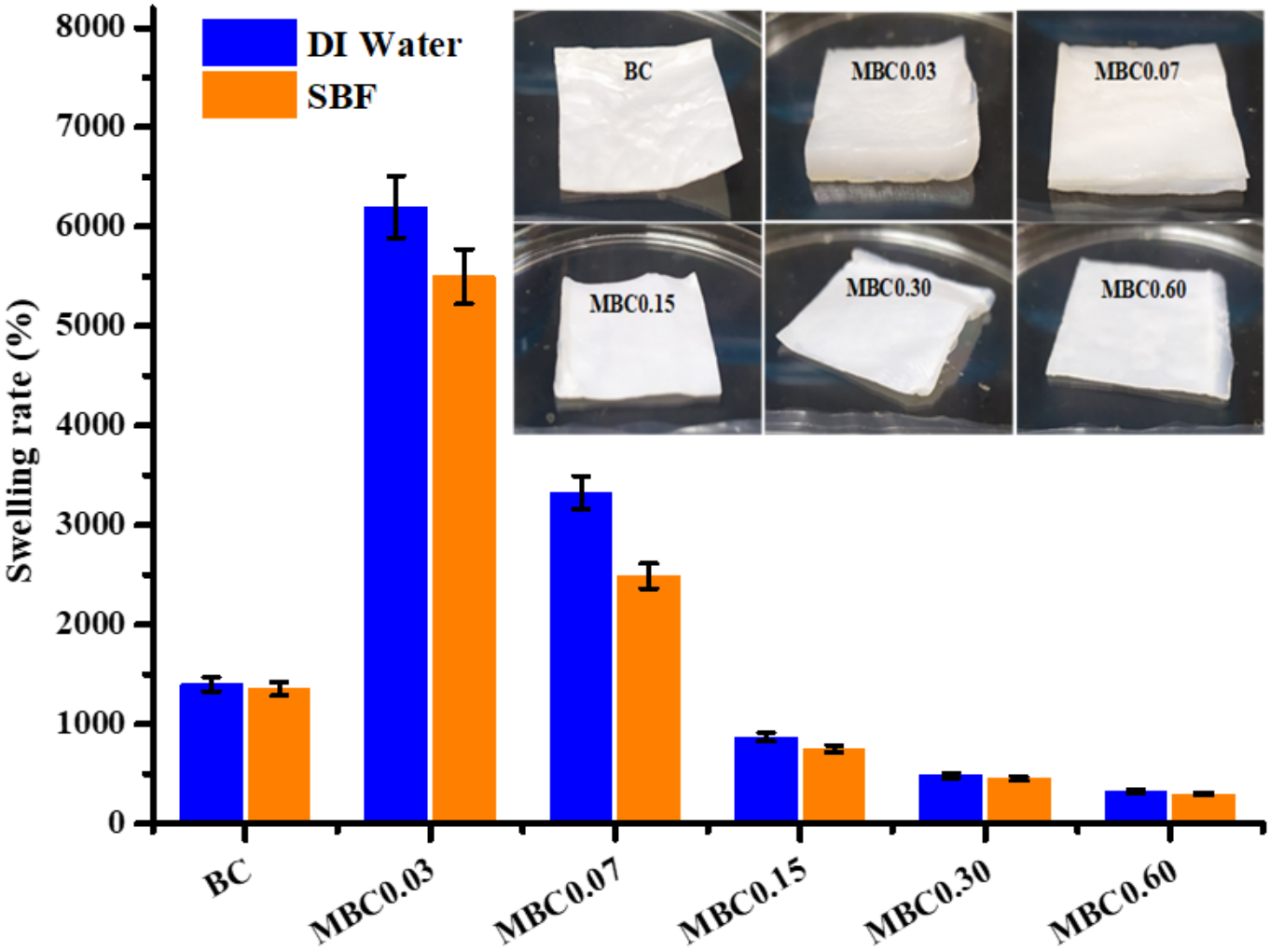

Figure 7

Swelling rates of the unmodified and modified BC in SBF and DI water

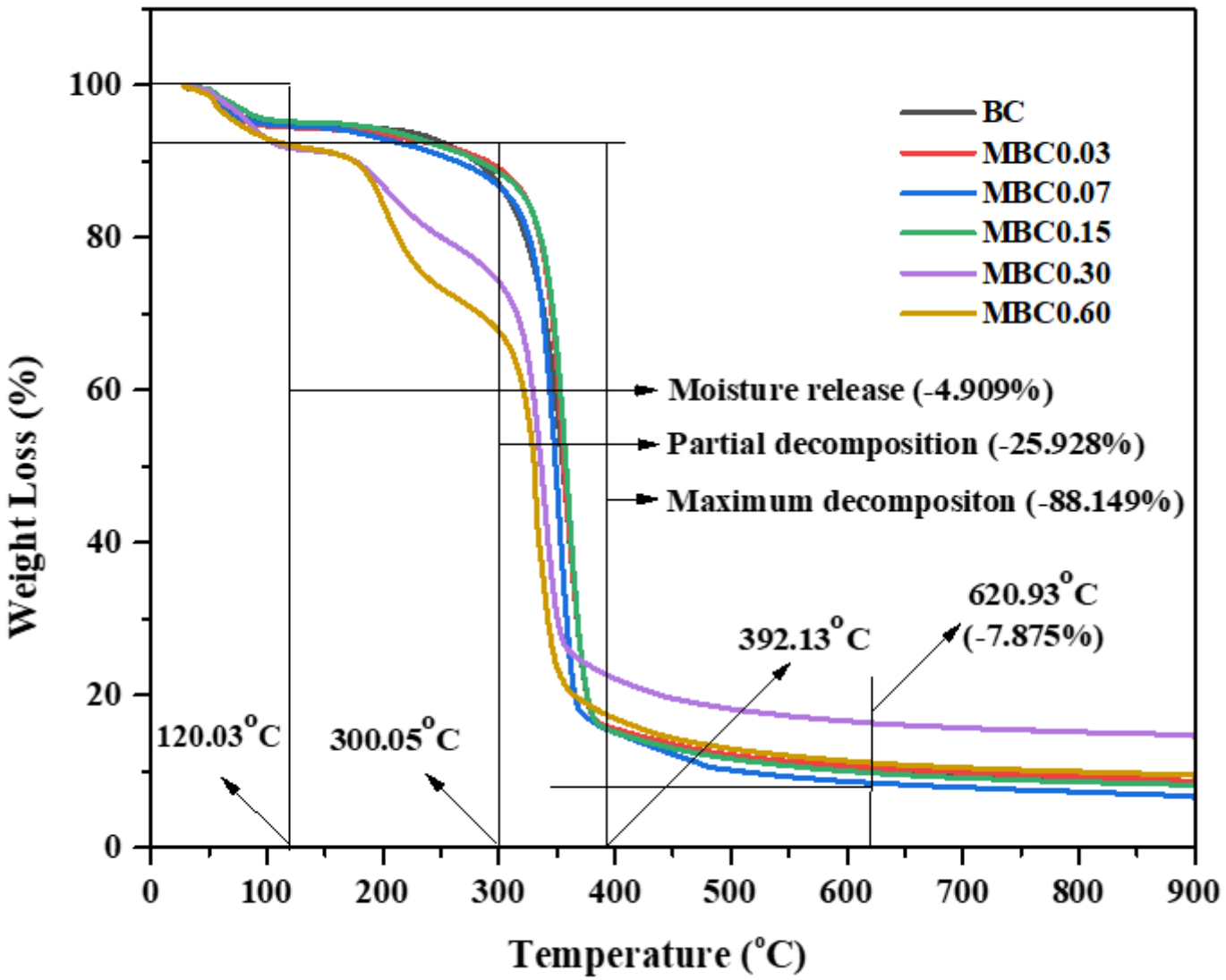

Figure 8

TGA graphs of the unmodified and modified BC samples

Supplementary Files

This is a list of supplementary files associated with this preprint. Click to download.

- GraphicalAbstract.docx